Acta Pharmacologica Sinica (2017) 38: 424–433
 1671-4083/17
www.nature.com/aps

Original Article

Soluplus micelles for improving the oral bioavailability of scopoletin and their hypouricemic effect *in vivo*

Ying-chun ZENG, Sha LI, Chang LIU, Tao GONG, Xun SUN, Yao FU*, Zhi-rong ZHANG*

Key Laboratory of Drug Targeting and Drug Delivery Systems, Ministry of Education, West China School of Pharmacy, Sichuan University, Chengdu 610041, China

Abstract

Scopoletin is an active coumarin possessing a variety of pharmacological activities, including anti-hyperuricemic effect, but with poor solubility. To improve its oral bioavailability, we attempted to encapsulate scopoletin into Soluplus micelles (Soluplus-based scopoletin micelles, Sco-Ms) and evaluated the hypouricemic action of Sco-Ms. Sco-Ms were prepared using a thin-film hydration method. Sco-Ms displayed near spherical shapes with an average size of 59.4±2.4 nm (PDI=0.08±0.02). The encapsulation efficiency of scopoletin was 87.3%±1.5% with a loading capacity of 5.5%±0.1%. Sco-Ms were further characterized using transmission electron microscopy, powder X-ray diffraction, Fourier transform infrared techniques and scanning electron microscopy. After oral administration in rats, Sco-Ms exhibited significantly improved absorption in each intestinal segment compared to free scopoletin, with the duodenum and jejunum being the main absorption regions. In rats administered Sco-Ms (at an equivalent dose of free scopoletin of 100 mg/kg, *po*), the $AUC_{0-\infty}$ and C_{max} of Sco-Ms were 4.38- and 8.43-fold, respectively, as large as those obtained following administration of free scopoletin. After oral administration in rats, Sco-Ms did not alter the tissue distributions of scopoletin, but significantly increased the scopoletin levels in the liver. In potassium oxonate-induced hyperuricemic mice, oral administration of Sco-Ms (at an equivalent dose of free scopoletin of 300 mg/kg) reduced the serum uric acid concentration to the normal level. The results suggest that Soluplus-based micelle system greatly improves the bioavailability of poorly water-soluble drugs, such as scopoletin, and represents a promising strategy for their oral delivery.

Keywords: scopoletin; Soluplus; micelles; oral bioavailability; pharmacokinetics; tissue distribution; hyperuricemic mice

Acta Pharmacologica Sinica (2017) 38: 424–433; doi: 10.1038/aps.2016.126; published online Jan 16 2017

Introduction

Scopoletin (6-methoxy-7-hydroxycoumarin, Figure 1) is a major active coumarin isolated from the stems of *Erycibe obtusifolia* Benth or *Erycibe schmidtii* Craib and is widely used to treat hemiplegia, rheumatoid arthritis, swelling and pain[1]. Scopoletin has been reported to show extensive pharmacologic actions, including anti-oxidative[2, 3], anti-thyroid[3], anti-hyperglycemic[3], anti-nociceptive[4] and anti-arthritic effects[5, 6]. In addition, scopoletin is a partially selective monoamine oxidase B inhibitor that increases the brain dopamine level[7]. Importantly, scopoletin has been extensively demonstrated to show remarkable anti-inflammatory[8–10], anti-hyperuricemic[11] and anti-gout effects[12]. Thus, scopoletin has been explored for gout therapy.

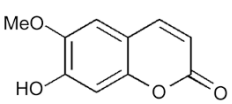

Figure 1. Chemical structure of scopoletin.

Oral administration is by far the most convenient and acceptable route of drug administration, especially for patients with chronic diseases who require long-term medication[13]. However, the absolute bioavailability of scopoletin is extremely low (approximately 6.0%)[14]. The poor bioavailability of scopoletin might be due to its low water solubility and instability in physiological media. As a result, most studies have used simple scopoletin suspensions and delivery via the parenteral route to achieve a pharmacological effect[11, 12]. Parenteral administration offers better bioavailability but has

*To whom correspondence should be addressed.
E-mail yfu4@scu.edu.cn (Yao FU);
zrzzl@vip.sina.com (Zhi-rong ZHANG)
Received 2016-08-19 Accepted 2016-10-12

obvious disadvantages, such as low levels of patient acceptance, safety concerns and high costs[15]. However, no oral formulations of scopoletin have been reported.

Polymeric micelles, with stable, biocompatible and solubilizing properties, have drawn considerable attention for the oral administration of poorly water-soluble drugs[16]. Soluplus, a polyvinyl caprolactam–polyvinyl acetate–polyethylene glycol (57/30/13) graft copolymer, is an amphipathic copolymer. Due to its high fluidity and excellent extrudability, Soluplus shows superior performance in forming solid solutions, especially in hot melt extrusion processes[17, 18]. As an amphiphile, Soluplus has been extensively used to improve the aqueous solubility and oral bioavailability of poorly soluble drugs[19], and it can self-assemble into micelles above the critical micelle concentration (CMC)[20].

In the present study, Soluplus-based micelles were applied for the first time to encapsulate scopoletin. We developed and characterized the optimized formulation of Soluplus-based micelles for scopoletin via the thin-film hydration method, and we aimed to assess its oral bioavailability, distribution and urate-lowering effect *in vivo*.

Materials and methods

Chemicals and reagents

Soluplus was kindly gifted by BASF SE (Ludwigshafen, Germany). Scopoletin (purity >98.0%) was purchased from Chengdu Jin Zhe Bio-tech Co, Ltd (Chengdu, China). Potassium oxonate was purchased from Nanjing Chemlin Chemical Industry Co, Ltd (China). Xanthine oxidase kits were provided by Jiancheng Bioengineering Institute (Nanjing, China).

Animals

All animal experiments were performed in accordance with the guidelines for animal experiments of Sichuan University (Chengdu, Sichuan, China). Male Sprague-Dawley rats (200±10 g) were obtained from the West China Experimental Animal Center of Sichuan University. ICR mice (22±2 g) were supplied by Chengdu Dossy Biological Technology Co, Ltd (Chengdu, China). Animals were raised in a controlled environment (temperature: 23–26 °C, relative humidity: 40%–60%, noise: <60 dB, 12 h dark-light cycle) for at least 1 week before the experiments to allow adaptation to the housing conditions. The animals were fasted for 12 h prior to the experiment with free access to water.

Sample preparation and solubility test

Sco-Ms were prepared according to the thin-film hydration technique. Briefly, mixtures of scopoletin and Soluplus with varying *w*/*w* ratios, such as 1:10, 1:15, 1:20 and 1:25, were dissolved in dichloromethane, followed by evaporation under reduced pressure in a rotary evaporator at 35 °C. Then, pure water was added to form scopoletin-encapsulated polymeric micelles. Finally, the micelle suspensions were filtered through a 0.45-μm polycarbonate membrane.

The water solubility was determined by shaking excess solute in water. Excess amounts of the Sco-Ms were dispersed in 2 mL of water and incubated in a shaking water bath at 25 °C for 48 h, until the solution was saturated with scopoletine. The supernatant was collected, filtered through a 0.45-μm membrane filter, and then diluted appropriately with methanol. The concentration of scopoletin was then determined by using a high performance liquid chromatography (HPLC) system equipped with an ultraviolet detector (Agilent Technologies, Santa Clara, CA, USA). Chromatographic separation was achieved on an octadecyl silica (ODS) column (Kromasil, 150 mm×4.6 mm, 5 μm) and the column temperature was 30 °C. The mobile phase consisted of (A) 0.05% (*v*/*v*) aqueous phosphoric acid and (B) acetonitrile (70/30, *v*/*v*). The flow rate was 1.0 mL/min and the detection wavelength was set at 346 nm.

Characterization of Sco-Ms

Particle size and morphology of Sco-Ms

The particle size and polydispersity index (PDI) of Sco-Ms were determined by dynamic light scattering using a Malvern Zetasizer NanoZS90 (Malvern Instruments, Malvern, UK). All experiments were repeated three times. The morphology of Sco-Ms was observed using a transmission electron microscope (TEM) (Tecnai G2F20, FEI, Eindhoven, The Netherlands). A dispersion of Sco-Ms was placed on a copper grid covered with nitrocellulose, negatively stained with 2% (*w*/*v*) phosphotungstic acid for 30 s, dried, and subjected to TEM observation.

Drug loading (DL) and drug entrapment efficiency (EE)

The content of scopoletin encapsulated in Sco-Ms was determined by the membrane ultrafiltration method. Encapsulation efficiency (EE) and drug-loading coefficient (DL) were calculated using the following formulas:

$$EE\% = \frac{W_e}{W_f} \times 100\% \quad (1)$$

$$DL\% = \frac{W_e}{W_m + W_f} \times 100\% \quad (2)$$

W_e is the weight of scopoletin measured in Sco-Ms, W_f is the weight of the feeding scopoletin, and W_m is the total weight materials added.

X-ray diffraction

The X-ray diffraction (XRD) patterns of powders, including scopoletin, Soluplus, physical mixtures of scopoletin and Soluplus (Sco-PM) and Sco-Ms, were recorded using an X-ray diffractometer (X'Pert Pro MPD, Philips, The Netherlands), using nickel-filtered Cu Ka radiation generated at 40 kV and 25 mA and a scanning rate of 2°/min over a 2θ range of 5–80°.

Fourier transform infrared spectrometry

The Fourier transform infrared (FTIR) spectra (Nicolet 6700, Thermo, Waltham, MA, USA) was used to characterize the possible interactions between the scopoletin and Soluplus in Sco-Ms. Five milligrams of each sample was lightly ground and mixed with KBr in the range of 500–4000 cm^{-1} with a resolution of 2 cm^{-1}.

Scanning electron microscopy

The surface morphology of scopoletin, Soluplus, Sco-PM and Sco-Ms was observed using a scanning electron microscope (SEM) (JSM-7500F scanning microscope, Tokyo, Japan) operated at 5.0 kV. The samples were mounted on a glass stub with double-sided adhesive tape and coated under vacuum with gold in an argon atmosphere prior to observation.

In vitro drug release

An *in vitro* Sco-Ms release study was performed using the dialysis bag method. Briefly, 2 mL of Sco-Ms (equivalent to 1 mg of scopoletin) was introduced into a dialysis membrane bag (molecular weight cutoff of 3.5 kDa, Solarbio Science & Technology Co, Beijing, People's Republic of China), and the end-sealed dialysis bag was incubated in 50 mL of release media at 37±0.5 °C and shaken at a speed of 100 r/min. Simulated gastric fluid (SGF) and simulated intestinal fluid (SIF) were used as the release media. At predetermined time intervals, 1 mL of the release media was withdrawn and replaced with an equal volume of the fresh solution (SGF or SIF). Then, 3 mL of methanol was added, and the sample was stored until HPLC analysis.

Absorption of Sco-Ms in the intestine

The absorption behavior of Sco-Ms and free scopoletin was measured in rats. Briefly, Sco-Ms and scopoletin suspensions were administered to the fasted rats at 100 mg/kg of scopoletin by oral gavage. At 15 min, 30 min, 60 min and 120 min after oral administration, the rats were sacrificed, and different intestinal segments of duodenum, jejunum, ileum and colon were removed. The selected intestinal segments were carefully rinsed with cold saline, accurately weighed, and homogenized with twice normal saline (0.9%, *w*/*v*) on a Precellys 24 lysis instrument (Bertin, France). Then, 300 μL of acetonitrile–methanol (2:1, *v*/*v*) was added to 100 μL of tissue homogenate. The mixture was vortexed for 3 min and centrifuged at 15 500×*g* for 10 min (Thermo Scientific Heraeus Biofuge Stratos, Osterode, Germany). The supernatant was analyzed by the HPLC method as described in the *Sample preparation and solubility test* section. The scopoletin concentration in each tissue was normalized by the weight of the selected intestinal segments.

To visualize the absorption of Sco-Ms in the intestine, Sco-Ms were fluorescently labeled with hydrophobic Nile red and orally administered to rats at 100 mg/kg scopoletin with 2.5 mg/kg of Nile red[21, 22]. At different time points, the rats were sacrificed, and different intestinal segments (duodenum, jejunum, ileum and colon) were isolated. The segments were gently washed by cold normal saline (pH 7.4), frozen at -30 °C in cryoembedding media (Zeta, SAKURA, Japan) and sectioned at 16 μm (MEV, SLEE, Germany). The sections were then fixed with 4% buffered paraformaldehyde and sequentially stained with DAPI (1 μg/mL, Sigma) before imaging by CLSM (Olympus, Japan).

Pharmacokinetic and biodistribution study

Male Sprague-Dawley rats (200±10 g) were fasted for 12 h before drug administration with free access to water. Scopoletin and Sco-PM suspensions were prepared by adding scopoletin or Sco-PM (1:15, *w*/*w*) to a 0.5% carboxymethylcellulose sodium (CMC-Na) solution and then ultrasonicated for several minutes to obtain homogenous suspensions. Three groups of rats were orally administered with scopoletin suspension, Sco-PM or Sco-Ms at an equivalent dose of 100 mg/kg scopoletin. The blood samples (approximately 0.3 mL) were collected via the orbital venous plexus at predetermined time intervals (2, 5, 10, 15, 20, 30, 45, 60, 90, and 120 min). All blood samples were immediately centrifuged at 3000×*g* for 5 min, and then the plasma supernatant was collected. The subsequent steps were identical to those of the intestine homogenates. The supernatant was collected and filtered through a 0.22-μm membrane. A liquid chromatography coupled with tandem mass spectrometry (LC-MS/MS, 6410B, Agilent Technologies, Santa Clara, CA, USA) was used to analyze the scopoletin. The HPLC system consisted of a rapid resolution liquid chromatography system (1200 series, Agilent Technologies, Santa Clara, CA, USA) equipped with an SL binary pump, SL autosampler and degasser. An Agilent 6410 triple-quadrupole mass spectrometer equipped with an electrospray ionization (ESI) interface was used for mass spectrometric analysis. The MS conditions were adjusted as previously reported[14]. The chromatographic separation was performed on a Diamonsil ODS column (100 mm×4.6 mm, 3 μm). The mobile phase consisted of (A) 0.1% (*v*/*v*) aqueous formic acid and (B) acetonitrile. The optimal gradient elution was programmed as follows: 0.0–2.5 min, 10.0%→85% B; 2.5–3.0 min, 85.0%→10.0% B; and 3.0–6.0 min, 10.0% B. The flow rate was 0.4 mL/min, and the column temperature was maintained at 30 °C.

Next, the biodistribution profiles of orally administered Sco-Ms and scopoletin suspension (dispersed in 0.5% CMC-Na) were compared. Rats were randomly divided into 2 groups (n=5) and orally administered with scopoletin suspension or Sco-Ms at an equivalent dose of 100 mg/kg. At the predetermined time points, the rats were sacrificed, and organs including the heart, liver, spleen, lung, kidney and brain were collected. The major organs were rinsed with cold physiological saline, accurately weighed and homogenized with twice normal saline (0.9%, *w*/*v*) on a Precellys 24 lysis instrument (Bertin, France). The subsequent sample pretreatment was performed as previously described. The scopoletin concentration in the supernatant was determined by HPLC and the biodistribution of scopoletin in each organ was normalized to the weight of the selected tissues.

Urate-lowering effect of Sco-Ms in hyperuricemic mice

Potassium oxonate, a uricase inhibitor, was used to induce hyperuricemia in mice according to a previous report[11]. Mice were randomly divided into five groups of eight each as follows: the normal group; hyperuricemic control group; scopoletin treated group; Sco-PM treated group; and Sco-Ms

treated group. Briefly, a oxonate suspension in 0.5% CMC-Na was intraperitoneally administered to mice at a dose of 350 mg/kg, whereas the mice in the normal group were injected with an equal volume of normal saline. After 1 h, the induced hyperuricemic mice were orally administered scopoletin suspension, Sco-PM suspension or Sco-Ms at an equivalent dose of 200 mg/kg scopoletin. The scopoletin suspension and Sco-PM suspension were prepared by dispersing them in 5% CMC-Na solution. The normal and hyperuricemic control group (non-treated) were both orally administered with the same volume of normal saline. After another hour, whole blood samples were collected and immediately centrifuged at 10000×g for 5 min to obtain the serum. The samples were stored at -20 °C for subsequent determination of uric acid level by an automatic biochemical analyzer (Hitachi 7020, Japan). Additionally, the livers were rapidly separated and washed by ice-cold normal saline followed by storage at -80 °C for the subsequent determination of hepatic xanthine oxidase (XOD) activity.

Statistical analysis

All data are expressed as the mean±standard deviation (SD). The statistical analysis was performed using Student's *t*-test for comparison between two groups. The difference was considered to be statistically significant at $P<0.05$ and very significant at $P<0.01$.

Results

Preparation of Sco-Ms and the solubility

Sco-Ms were prepared by the thin-film hydration technique (Figure 2A). Table 1 shows the water solubility of scopoletin in Sco-Ms and Sco-PM. For Sco-PM, the solubility of scopoletin increased slightly with increasing of Soluplus, mainly due to the solubilization effect of Soluplus[23]. Scopoletin in different Sco-Ms formulations displayed water solubilities over 7.900 mg/mL, which were significantly higher than the corresponding Sco-PM of the same scopoletin to Soluplus weight ratio. In addition, Sco-Ms formulation with 1:15 (*w*/*w*) scopoletin/Soluplus achieved a saturated solubility of 8.512 mg/mL and appeared to reach saturation in the solubility test, whereas the solubility of scopoletin did not further increase when increasing the percentage of Soluplus. Thus, Sco-Ms with a drug/Soluplus ratio (*w*/*w*) of 1:15 were selected for subsequent study.

Table 1. Solubility of scopoletin, Sco-PM, and Sco-Ms in water at 25 °C. Data represent mean±SD. *n*=3.

Scopoletin/ Soluplus (*w*/*w*)	Sco-PM (mg/mL)	Sco-Ms (mg/mL)
1:0	0.259±0.003	NA
1:10	1.156±0.034	7.900±0.050
1:15	1.450±0.029	8.512±0.073
1:20	1.461±0.116	8.381±0.161
1:25	1.798±0.094	8.477±0.060

Note: NA, not available

Characterization of Sco-Ms

Particle size and morphology of Sco-Ms

The average particle size and the PDI of Sco-Ms were studied by dynamic light scattering. The representative size distribution of Sco-Ms clearly showed a narrow size distribution with an average particle diameter of 59.4±2.4 nm (PDI=0.08±0.02) (Figure 2B). The TEM image showed that Sco-Ms displayed a

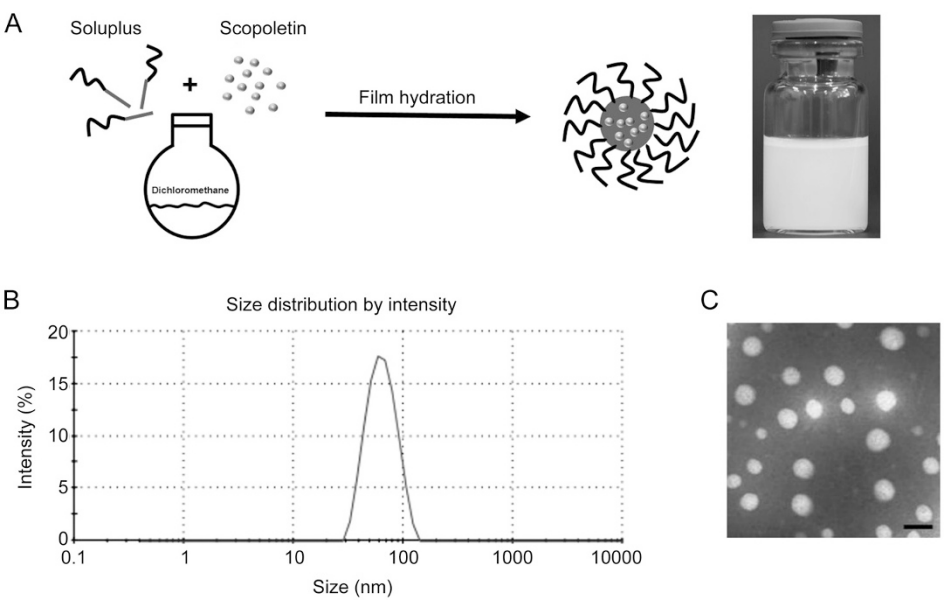

Figure 2. Preparation and characterization of Sco-Ms. (A) Scheme of the preparation of Sco-Ms. (B) Size distribution of Sco-Ms by intensity. (C) Representative TEM image of Sco-Ms, scale bar represents 100 nm.

near-spherical morphology (Figure 2C).

Drug loading (DL) and drug entrapment efficiency (EE)

In our study, the ultrafiltration method was used to study the entrapment efficiency. The interception molecular weight of the ultrafiltration membrane was 3 kDa. The free drug could pass through the ultrafiltration membrane, whereas scopoletin encapsulated into Soluplus micelles could not. The encapsulation efficiency and drug loading of scopoletin in Sco-Ms were 87.3%±1.5% and 5.5%±0.1%, respectively.

X-ray diffraction

Scopoletin is a highly crystalline molecule with main characteristic crystalline peaks at 12.52, 13.26, 16.54, 19.09, 23.66, 25.18, 26.44, and 30.80 θ degrees (Figure 3A). The physical mixture of scopoletin and Soluplus also presented a number of distinct peaks, indicating that scopoletin was crystalline in the mixture. By contrast, the characteristic peaks of scopoletin were absent in Sco-Ms, suggesting a conversion of the crystalline form of scopoletin to the amorphous form.

Fourier transform infrared spectroscopy

The possible molecular interactions within the solid matrix of the PMs were examined by FTIR (Figure 3B). Scopoletin displayed –OH stretching at 3337 cm^{-1}, carbonyl stretching for cyclic esters (lactone) at 1703 cm^{-1}, $-CH_3$ at 2992 cm^{-1} and 1379 cm^{-1}, and benzene stretching at 3022 cm^{-1}, 1609 cm^{-1} and 1509 cm^{-1} (Figure S1). Soluplus showed inter-molecularly hydro-

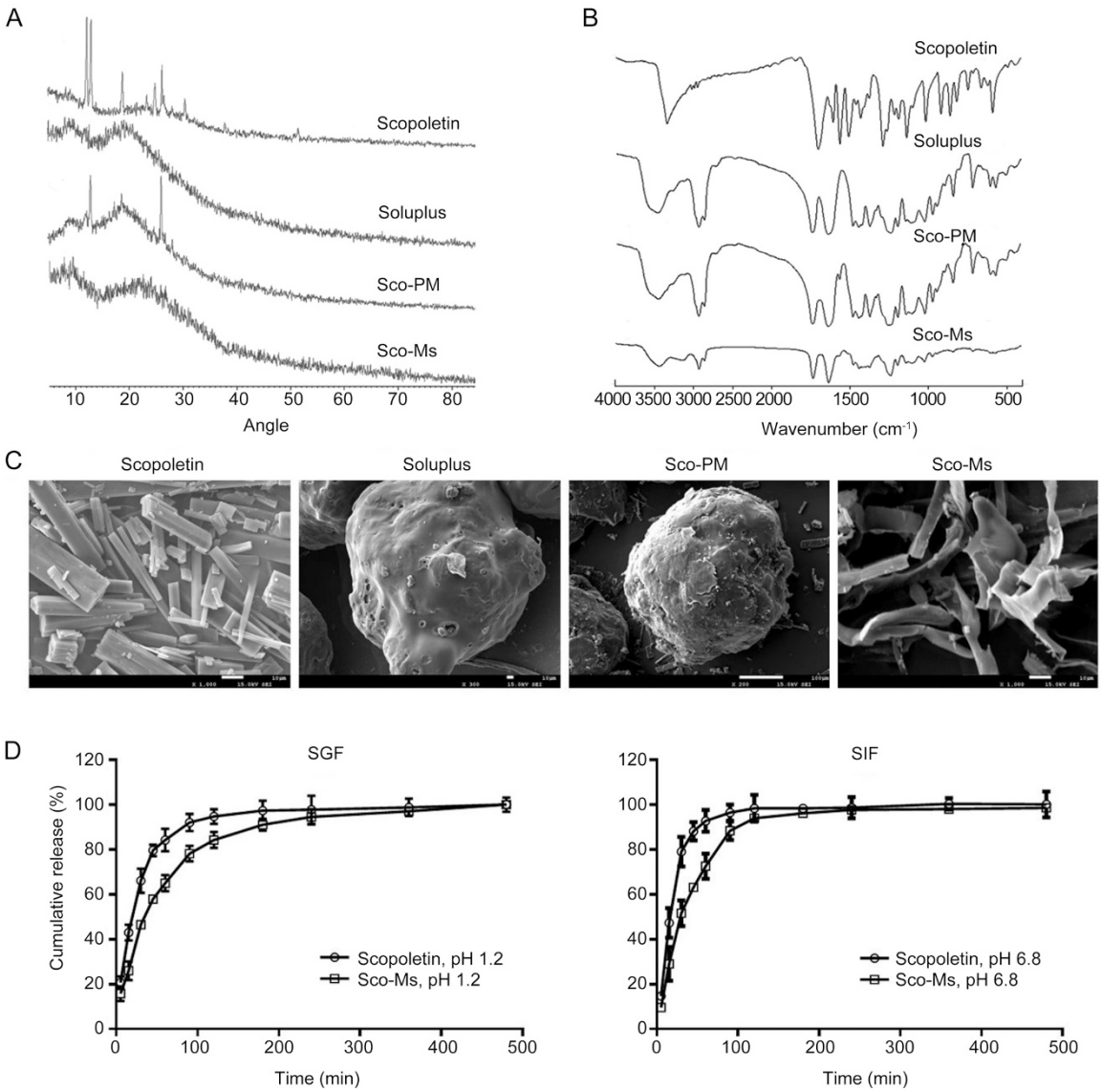

Figure 3. Characterization of Sco-Ms. (A) X-ray diffractograms of scopoletin, Soluplus, Sco-PM and Sco-Ms. (B) Fourier transform infrared spectroscopy (FTIR) of scopoletin, Soluplus, Sco-PM and Sco-Ms. (C) Scanning electron micrographs (SEM) of scopoletin, Soluplus, Sco-PM and Sco-Ms. Scale bars represent 10 μm, 10 μm, 100 μm and 10 μm, respectively. (D) *In vitro* release profiles of free scopoletin and Sco-Ms in SGF (pH 1.2) and SIF (pH 6.8). Data represent mean±SD. *n*=3.

gen bonded –OH stretching in the range of 3456–3268 cm^{-1}, ester carbonyl stretching 1740–1640 cm^{-1}, and C=O stretching for tertiary amides at 1740 cm^{-1} (Figure S2). No spectral shift was found in the Sco-PM, which was a simple superposition of scopoletin and Soluplus, indicating no interactions between the drug and polymer (Figure S3). However, in the FTIR spectrum of Sco-Ms, the –OH stretching peaks of scopoletin and Soluplus appeared at 3436 cm^{-1} and became slightly broader, and the position of C=O absorption peaks was shifted to 1736 cm^{-1} and 1637 cm^{-1} (Figure S4), indicating that Soluplus might interact with scopoletin by forming intermolecular hydrogen bonds.

Scanning electron microscopy

As for the surface morphology, the SEM image of bulk scopoletin presented large, inerratic clavate crystals (Figure 3C). By contrast, Sco-Ms displayed flake-like morphology and no scopoletin crystals were observed (Figure 3C).

In vitro release kinetics

To simulate the *in vivo* biological environment, the *in vitro* release profiles of scopoletin were characterized under a pH gradient simulating the pH evolution of the GI tract (SGF, pH 1.2; SIF, pH 6.8). As shown in Figure 3D, the cumulative release percentages of scopoletin from free scopoletin and Sco-Ms were both near 100% in SGF/SIF by 8 h, whereas a lower release rate of scopoletin was observed in SGF than in SIF. Sco-Ms showed more sustained release of scopoletin both in SGF and SIF compared to free scopoletin, which is likely due to the formation of hydrogen bonds between drug molecules and the polymer.

Absorption of Sco-Ms in the intestine

The intestinal absorption of Sco-Ms in each intestinal segment was different, and varied over time after oral administration. At 15 min and 30 min after oral administration, the tissue concentration of Sco-Ms remained the highest in the duodenum and jejunum, and gradually decreased from the ileum to the colon (Figure 4A and 4B). Then, the scopoletin concentration from Sco-Ms in the duodenum and jejunum declined over time, whereas the scopoletin concentration in the ileum and colon reached the highest level at 60 min and then gradually decreased (Figure 4C). The absorption of Sco-Ms in the intestine could be affected by the gastric emptying rate and forces, GI hydrodynamics, intestinal transit time and flow rate. Compared to free scopoletin, the scopoletin concentration from Sco-Ms was significantly improved in the intestine.

To visualize the intestinal absorption of Sco-Ms, Nile red labeled scopoletin was orally administered to rats. Thirty minutes after administration, the red fluorescence was substantially greater in the jejunum and duodenum, whereas little red fluorescence was observed in ileum and colon (Figure 5). After 60 min, the red fluorescence became weaker in the duodenum and jejunum, whereas strong red fluorescence hardly appeared in ileum and colon (Figure 5). The CLSM images further suggested that Sco-Ms were rapidly absorbed after

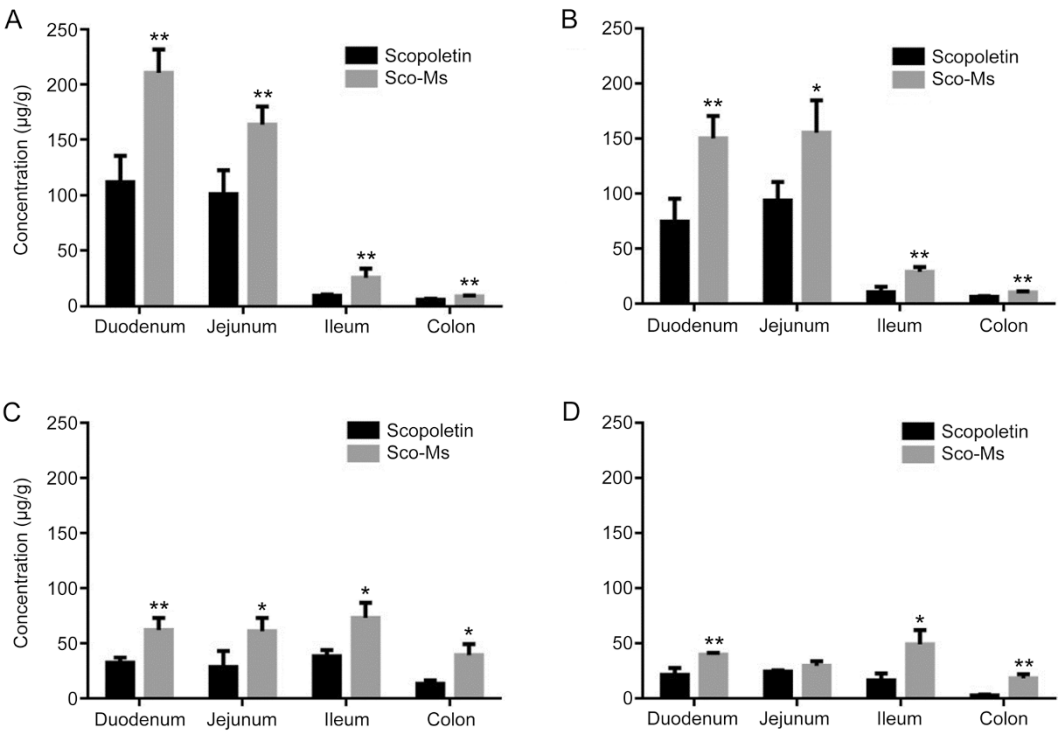

Figure 4. Absorption of Sco-Ms in the intestine at different time points after oral administration in rats. (A) 15 min; (B) 30 min; (C) 60 min; (D) 120 min. Data represent mean±SD. n=5. $^{*}P$<0.05, $^{**}P$<0.01 *vs* scopoletin.

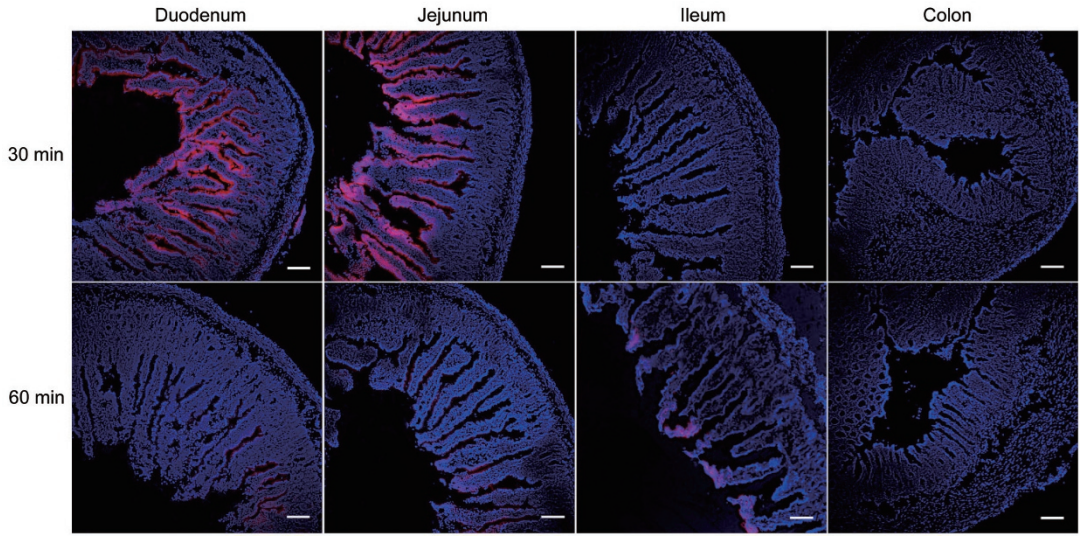

Figure 5. Intestinal absorption of Nile red labeled Sco-Ms at 100 mg/kg scopoletin with 2.5 mg/kg Nile red after oral adiministration under CLSM. Nuclei were stained with DAPI (blue). Scale bars represent 100 μm.

oral administration and were mainly absorbed in the proximal intestine, which was in accordance with the quantitative results.

Pharmacokinetics and biodistribution

The plasma concentration–time profiles of scopoletin in healthy Sprague-Dawley rats following oral administration of scopoletin, Sco-PM and Sco-Ms are presented in Figure 6. The pharmacokinetic parameters of scopoletin in each group are given in Table 2. Scopoletin and the Sco-PM suspension showed similar intracorporal processes, whereas Sco-Ms displayed a pharmacokinetic profile dramatically different from that of free scopoletin or Sco-PM. Specifically, Sco-Ms showed significantly higher C_{max} values than scopoletin and Sco-PM (P<0.01) (Table 2). Approximately 4.38-fold and 4.44-fold increases in the $AUC_{0-\infty}$ values were observed for Sco-Ms compared to the scopoletin and Sco-PM suspension (P<0.01), respectively.

As shown in Figure 7, scopoletin was distributed mainly in the liver, spleen, lung and kidney following the oral administration of the scopoletin suspension and Sco-Ms, indicating that Sco-Ms did not alter the main distribution sites of scopoletin. The distribution of scopoletin in the brain was limited, and it could not be detected after 60 min following oral administration. Importantly, Sco-Ms exhibited a much higher scopoletin concentration in liver than the scopoletin suspension (Figure 7), which would be highly beneficial for the inhibition

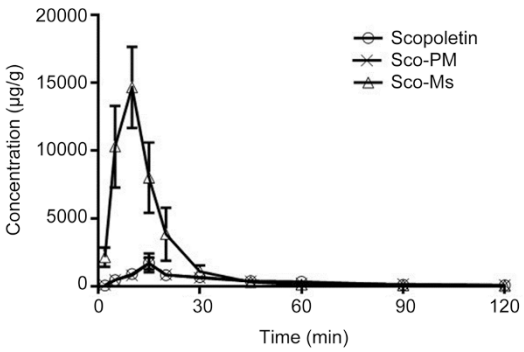

Figure 6. Plasma concentration-time profiles of free scopoletin, Sco-PM and Sco-Ms after oral administration in rats. Data represent mean±SD. n=5.

Table 2. Pharmacokinetic parameters of scopoletin in rats. Data represent mean±SD. n=5. $^{**}P$<0.01 *vs* scopoletin.

Parameter	Scopoletin	Sco-PM	Sco-Ms
AUC_{0-t} (μg·h/L)	770.766±56.664	722.856±102.191	3513.596±469.089**
$AUC_{0-\infty}$ (μg·h/L)	805.725±62.801	794.763±124.936	3529.586±471.201**
MRT_{0-t} (h)	0.590±0.048	0.598±0.069	0.244±0.015**
$MRT_{0-\infty}$ (h)	0.683±0.091	0.800±0.132	0.255±0.021**
$t_{1/2}$ (h)	0.476±0.141	0.592±0.105	0.468±0.138
T_{max} (h)	0.266±0.036	0.250±0.000	0.167±0.000**
CL ($L{\cdot}h^{-1}{\cdot}kg^{-1}$)	124.715±9.678	128.289±19.801	28.703±3.482**
C_{max} (μg/L)	1741.416±657.213	1668.506±438.995	14674.796±2997.147**

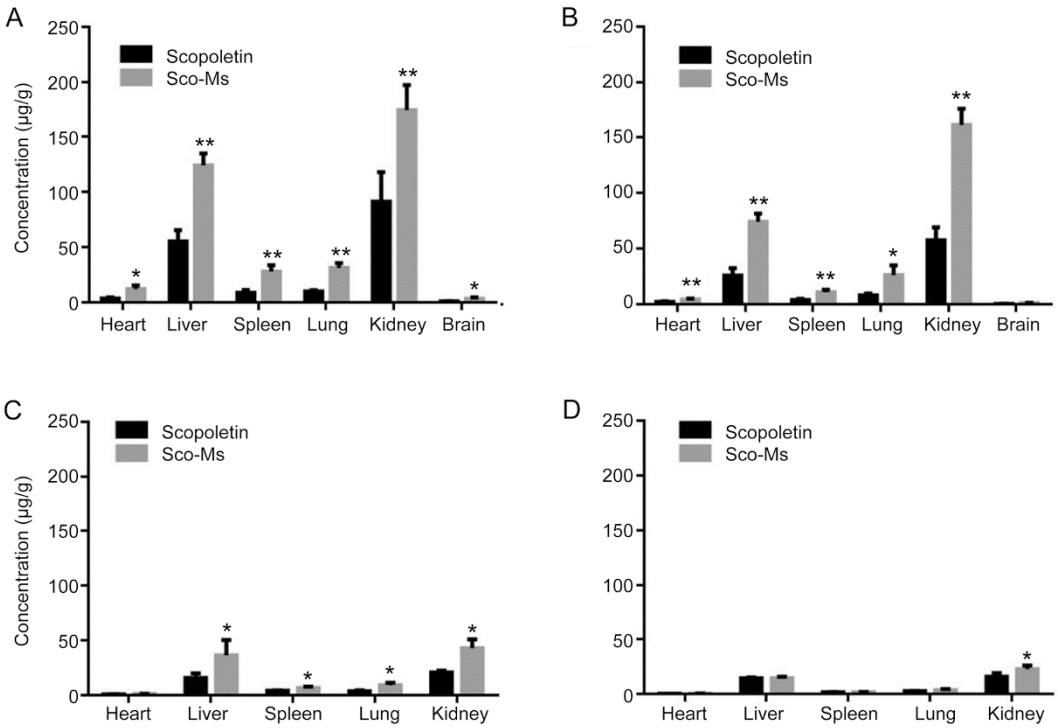

Figure 7. Biodistribution of Sco-Ms at different time points after oral administration in rats. (A) 15 min; (B) 30 min; (C) 60 min; (D) 120 min. Data represent mean±SD. n=5. $^{*}P$<0.05, $^{**}P$<0.01 *vs* scopoletin.

of hepatic XOD activity.

Urate-lowering effect of Sco-Ms in hyperuricemic mice

As shown in Figure 8, the uric acid level in the serum was significantly increased after the injection of potassium oxonate (350 mg/kg), indicating that a hyperuricemia model in mice was successfully established. Sco-Ms administered orally significantly reduced the serum uric acid levels of hyperuricemic mice, whereas scopoletin and Sco-PM showed no obvious effect on the serum uric acid levels.

To investigate the possible mechanism of the anti-hyperuricemic effect of Sco-Ms, the hepatic and serum XOD activity of hyperuricemic rats under different treatments were assessed.

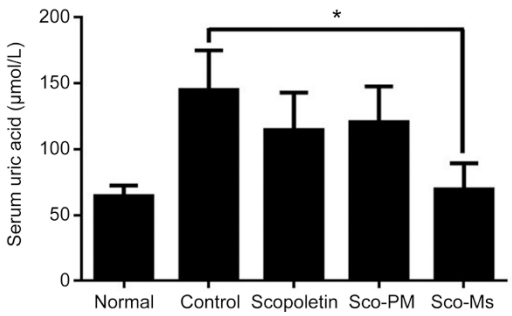

Figure 8. Urate-lowering effect of Sco-Ms in hyperuricemic mice. Data represent mean±SD. n=8. $^{*}P$<0.05 *vs* control.

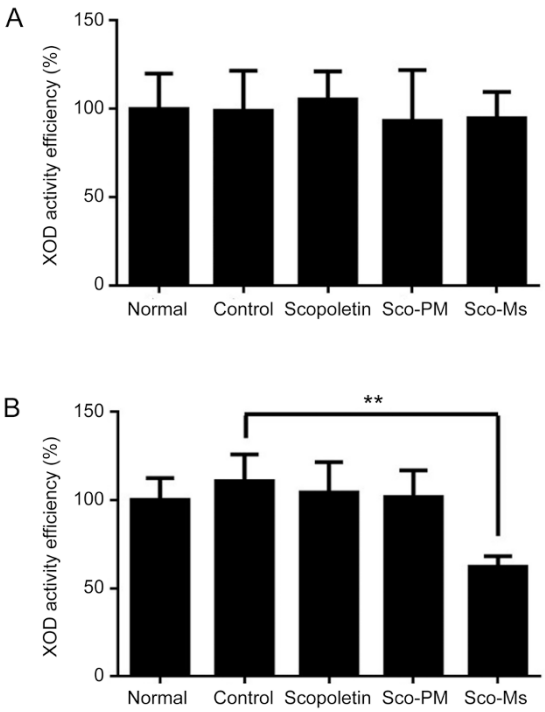

Figure 9. Inhibitory effect of Sco-Ms on xanthine oxidase activity (XOD) in mice serum (A) and liver (B). The XOD activity of normal group was set as 100%. Results were presented as mean±SD. n=8. $^{**}P$<0.01 *vs* control.

No significant differences were observed for the serum XOD activity of normal and control (P>0.05), indicating that the potassium oxonate treatment did not affect the serum XOD activity of mice (Figure 9A). Similarly, the hepatic XOD activity of mice remained unchanged after potassium oxonate treatment (Figure 9B). Moreover, scopoletin and Sco-PM did not show inhibitory effects either on the hepatic or the serum XOD activity. However, compared to the control, Sco-Ms significantly decreased hepatic XOD activity. In addition, no significantly reduced serum XOD activity was observed for Sco-Ms, suggesting that the anti-hyperuricemic effect of Sco-Ms was due to inhibition of hepatic XOD activity, rather than inhibition of serum XOD activity, thus leading to the decreased serum uric acid level.

Discussion

Soluplus has numerous advantages, such as amphiphilicity, minimum toxicity and low hygroscopicity, and has been used in a variety of pharmaceutical technologies, including the generation of micelles[24], solid dispersions[25], nanoparticles[26] and self-emulsifying drug delivery systems[27]. Soluplus has been proven to possess the potential to increase the solubility and bioavailability of a number of poorly water-soluble compounds, such as itraconazole[28], osthole[29], fenofibrate[30] and sorafenib[31]. In the current study, the Soluplus-based micelle system was applied for the first time to scopoletin.

Using solubility as an optimization standard, we optimized the ratio (w/w) of scopoletin and Soluplus. Scopoletin was only slightly soluble in water (~0.259 mg/mL in distilled water at 25 °C), whereas Sco-Ms with 1:15 (w/w) of scopoletin/Soluplus achieved a saturated scopoletin solubility of 8.512 mg/mL. As demonstrated by XRD, FTIR and SEM analysis, scopoletin formed intermolecular hydrogen bonding with the carriers and was encapsulated in micelles, thus resulting in the greatly increased solubility of scopoletin. Sco-Ms displayed near-spherical uniform particles with an average size distribution of approximately 60 nm. The low polydispersity index indicated the uniformity of the size of the micelles.

Compared to the free scopoletin, Sco-Ms significantly improved the intestinal absorption, bioavailability and tissue distribution of scopoletin. The following reasons may explain the differences between the two groups. First, Sco-Ms significantly changed the dissolution characteristics of scopoletin, and the solubility of scopoletin was improved by approximately 33 times. High dissolution is beneficial for drug absorption. Second, because of the viscosity properties of Sco-Ms, the Sco-Ms could adhere to the intestines and increase the contact area and contact time between the drug and GI tract, which contributed to the enhanced absorption of scopoletin. Third, studies have reported that nanoparticles with sizes approximately at or below 100 nm show optimum cellular and nuclear uptake in smooth muscle and epithelial cells[20, 32]. In addition, another previous study indicated that phase II metabolism might be one of the reasons for the poor bioavailability of scopoletin[14]. Glucuronide and sulfate conjugates of scopoletin were detected in plasma samples after oral administration. Scopoletin encapsulated in the Sco-Ms would reduce the degradation and metabolism when in contact with GI contents.

Researchers have found that scopoletin exhibits a hypouricemic effect after intraperitoneal administration in mice with potassium oxonate-induced hyperuricemia[11]. One of the reasons was that scopoletin could inhibit xanthine oxidase in the liver. After the mice were orally administered Sco-Ms, the significantly increased scopoletin concentrations in liver (Figure 7) suggested that Sco-Ms may have superior anti-hyperuricemic effects *in vivo* than scopoletin. To prove our hypothesis, we conducted pharmacological studies using the same hyperuricemia mouse model. Sco-Ms reduced the high serum uric acid level to normal in hyperuricemic mice after hyperuricemia was induced for 2 h (Figure 8). We demonstrated that Sco-Ms could achieve its urate-lowering effect by inhibiting the hepatic XOD activity after oral administration. By contrast, free scopoletin showed no therapeutic effect on hyperuricemic mice at the test dose. This result may be due to the low oral absorption of scopoletin, which was not sufficient to achieve satisfactory therapeutic efficiency.

Conclusion

In the present study, Soluplus-based scopoletin micelles were successfully prepared using the thin-film hydration method. The solubility of the scopoletin in the micelles was approximately 33 times higher than the solubility of free scopoletin in water. The pharmacokinetic and biodistribution study demonstrated that Sco-Ms displayed much higher oral bioavailability and tissue concentrations compared to free scopoletin in rats. Moreover, Sco-Ms was shown to have improved therapeutic efficacy in hyperuricemic mice, which may also be translated to other applications such as the treatment of tumors and cancer via the oral route of administration[33]. Thus, Soluplus-based micelles represents a highly promising approach to improving the oral bioavailability of poorly water-soluble drugs and to achieve better therapeutic effects *in vivo*.

Author contribution

Zhi-rong ZHANG and Ying-chun ZENG conceived and designed the study. Ying-chun ZENG performed the experiments, generated laboratory data, conducted preliminary analysis of the data and wrote the initial article. Sha LI and Chang LIU assisted in the animal experiments. Tao GONG, Xun SUN, Yao FU and Ying-chun ZENG assisted in data analysis, manuscript writing and editing. All authors reviewed the manuscript.

Acknowledgements

This work was funded by the National S&T Major Project of China (No 2011ZX09310-002) and the National Natural Science Foundation of China (No 81130060).

Supplementary information

Supplementary information is available at the website of Acta Pharmacologica Sinica.

References

1 The state pharmacopoeia commission of the PR China. Pharmacopoeia of the PR China. China Medical Science Press: Beijing; 2010. p 3–4.
2 Shaw CY, Chen CH, Hsu CC, Chen CC, Tsai YC. Antioxidant properties of scopoletin isolated from *Sinomonium acutum*. Phytother Res 2003; 17: 823–5.
3 Panda S, Kar A. Evaluation of the antithyroid, antioxidative and antihyperglycemic activity of scopoletin from *Aegle marmelos* leaves in hyperthyroid rats. Phytother Res 2006; 20: 1103–5.
4 Ardenghi JV, Pretto JB, Souza MM, Junior AC, Soldi C, Pizzolatti MG, *et al.* Antinociceptive properties of coumarins, steroid and dihydrostyryl-2-pyrones from *Polygala sabulosa* (Polygalaceae) in mice. J Pharm Pharmacol 2006; 58: 107–12.
5 Pan R, Gao XH, Li Y, Xia YF, Dai Y. Anti-arthritic effect of scopoletin, a coumarin compound occurring in *Erycibe obtusifolia* Benth stems, is associated with decreased angiogenesis in synovium. Fundam Clin Pharmacol 2010; 24: 477–90.
6 Romero-Cerecero O, Meckes-Fischer M, Zamilpa A, Jiménez-Ferrer JE, Nicasio-Torres P, Pérez-García D, *et al.* Clinical trial for evaluating the effectiveness and tolerability of topical *Sphaeralcea angustifolia* treatment in hand osteoarthritis. J Ethnopharmacol 2013; 147: 467–73.
7 Basu M, Mayana K, Xavier S, Balachandran S, Mishra N. Effect of scopoletin on monoamine oxidases and brain amines. Neurochem Int 2016; 93: 113–7.
8 Kim HJ, Jang SI, Kim YJ, Chung HT, Yun YG, Kang TH, *et al.* Scopoletin suppresses pro-inflammatory cytokines and PGE2 from LPS-stimulated cell line, RAW 264.7 cells. Fitoterapia 2004; 75: 261–6.
9 Moon PD, Lee BH, Jeong HJ, An HJ, Park SJ, Kim HR, *et al.* Use of scopoletin to inhibit the production of inflammatory cytokines through inhibition of the IkappaB/NF-kappaB signal cascade in the human mast cell line HMC-1. Eur J Pharmacol 2007; 555: 218–25.
10 Ding ZQ, Dai Y, Hao HP, Pan R, Yao XJ, Wang ZT. Anti-inflammatory effects of scopoletin and underlying mechanisms. Pharm Biol 2008, 46: 854–60.
11 Ding Z, Dai Y, Wang Z. Hypouricemic action of scopoletin arising from xanthine oxidase inhibition and uricosuric activity. Planta Med 2005; 71: 183–5.
12 Yao X, Ding Z, Xia Y, Wei Z, Luo Y, Feleder C, *et al.* Inhibition of monosodium urate crystal-induced inflammation by scopoletin and underlying mechanisms. Int Immunopharmacol 2012; 14: 454–62.
13 Lavelle E, Sharif S, Thomas N, Holland J, Davis S. The importance of gastrointestinal uptake of particles in the design of oral delivery systems. Adv Drug Delivery Rev 1995; 18: 5–22.
14 Zeng Y, Li S, Wang X, Gong T, Sun X, Zhang Z. Validated LC-MS/MS method for the determination of Scopoletin in rat plasma and its application to pharmacokinetic studies. Molecules 2015; 20: 18988–9001.
15 Ko KT, Needham TE, Zia H. Emulsion formulations of testosterone for nasal administration. J Microencapsul 1998; 15: 197–205.
16 Bromberg L. Polymeric micelles in oral chemotherapy. J Control Release 2008; 128: 99–112.
17 Potter C, Tian Y, Walker G, McCoy C, Hornsby P, Donnelly C, *et al.* Novel supercritical carbon dioxide impregnation technique for the production of amorphous solid drug dispersions: a comparison to hot melt extrusion. Mol Pharm 2015; 12: 1377–90.
18 Khinast J, Baumgartner R, Roblegg E. Nano-extrusion: a one-step process for manufacturing of solid nanoparticle formulations directly from the liquid phase. AAPS PharmSciTech 2013; 14: 601–4.
19 Linn M, Collnot EM, Djuric D, Hempel K, Fabian E, Kolter K, *et al.* Soluplus® as an effective absorption enhancer of poorly soluble drugs *in vitro* and *in vivo*. Eur J Pharm Sci 2012; 45: 336–43.
20 Dian L, Yu E, Chen X, Wen X, Zhang Z, Qin L, *et al.* Enhancing oral bioavailability of quercetin using novel soluplus polymeric micelles. Nanoscale Res Lett 2014; 9: 1–11.
21 Gao F, Zhang Z, Bu H, Huang Y, Gao Z, Shen J, *et al.* Nanoemulsion improves the oral absorption of candesartan cilexetil in rats: Performance and mechanism. J Control Release 2011; 149: 168–74.
22 Zhang Z, Ma L, Jiang S, Liu Z, Huang J, Chen L, *et al.* A self-assembled nanocarrier loading teniposide improves the oral delivery and drug concentration in tumor. J Control Release 2013; 166: 30–7.
23 Lin Q, Fu Y, Li J, Qu M, Deng L, Gong T, *et al.* A (polyvinyl caprolactam-polyvinyl acetate-polyethylene glycol graft copolymer)-dispersed sustained-release tablet for imperialine to simultaneously prolong the drug release and improve the oral bioavailability. Eur J Pharm Sci 2015; 79: 44–52.
24 Yu HZ, Xia DN, Zhu QL, Zhu CL, Chen D, Gan Y. Supersaturated polymeric micelles for oral cyclosporine A delivery. Eur J Pharm Biopharm 2013; 85: 1325–36.
25 Lian X, Dong J, Zhang J, Teng Y, Lin Q, Fu Y, *et al.* Soluplus® based 9-nitrocamptothecin solid dispersion for peroral administration: preparation, characterization, *in vitro* and *in vivo* evaluation. Int J Pharm 2014; 477: 399–407.
26 Jog R, Kumar S, Shen J, Jugade N, Tan DC, Gokhale R, *et al.* Formulation design and evaluation of amorphous ABT-102 nanoparticles. Int J Pharm 2016; 498: 153–69.
27 Lee DH, Yeom DW, Song YS, Cho HR, Choi YS, Kang MJ, *et al.* Improved oral absorption of dutasteride via Soluplus®-based supersaturable self-emulsifying drug delivery system (S-SEDDS). Int J Pharm 2015; 478: 341–7.
28 Zhang K, Yu H, Luo Q, Yang S, Lin X, Zhang Y, *et al.* Increased dissolution and oral absorption of itraconazole/Soluplus extrudate compared with itraconazole nanosuspension. Eur J Pharm Biopharm 2013; 85: 1285–92.
29 Yun F, Kang A, Shan J, Zhao X, Bi X, Li J, *et al.* Preparation of ostholepolymer solid dispersions by hot-melt extrusion for dissolution and bioavailability enhancement. Int J Pharm 2014; 465: 436–43.
30 Yang H, Teng F, Wang P, Tian B, Lin X, Hu X, *et al.* Investigation of a nanosuspension stabilized by Soluplus® to improve bioavailability. Int J Pharm 2014; 477: 88–95.
31 Truong, DH, Tran TH, Ramasamy T, Choi JY, Choi HG, Yong CS, *et al.* Preparation and characterization of solid dispersion using a novel amphiphilic copolymer to enhance dissolution and oral bioavailability of sorafenib. Powder Technol 2015, 283: 260–5.
32 Feng SS, Mei L, Anitha P, Gan CW, Zhou W. Poly(lactide)-vitamin E derivative/montmorillonite nanoparticle formulations for the oral delivery of docetaxel. Biomaterials 2009; 30: 3297–306.
33 Tabana YM, Hassan LE, Ahamed MB, Dahham SS, Iqbal MA, Saeed MA, *et al.* Scopoletin, an active principle of tree tobacco (Nicotiana glauca) inhibits human tumor vascularization in xenograft models and modulates ERK1, VEGF-A, and FGF-2 in computer model. Microvasc Res 2016; 107: 17–33.